

Electronic Supplementary Information

Fe and P dual-doped nickel carbonate hydroxide/carbon nanotube hybrid electrocatalyst for efficient oxygen evolution reaction

*Qing Ye¹, Jiang Liu¹, Lu Lin, Min Sun, Yufeng Wang and Yongliang Cheng**

Key Laboratory of Synthetic and Natural Functional Molecule of the Ministry of Education, College of Chemistry and Materials Science, Northwest University, Xi'an 710069, China

[1] These authors contributed equally to this work

* Corresponding authors: ylcheng@nwu.edu.cn (Y.L. Cheng)

Experimental section

Calculation methods

All calculations were performed with spin-polarization density functional theory (DFT). The generalized gradient approximation (GGA) using the Perdew-Burke-Ernzerhof (PBE) formulation was employed to describe the electron exchange correlation interaction. The ionic cores were described by the projected augmented wave (PAW) potentials. The plane wave basis set was 500 eV. Partial occupancies of the Kohn–Sham orbitals were allowed using the Gaussian smearing method and a width of 0.05 eV. The convergence criteria of electronic energy and geometry optimization were set to 10^{-4} eV and 0.05 eV Å⁻¹, respectively. The vacuum spacing in a direction perpendicular to the plane of the structure is 16 Å. The Brillouin zone integration is performed using 3×3×1 Monkhorst-Pack k-point. The U correction for Ni and Fe atoms was set as 3.75 and 4.34 eV, respectively. Additionally, the density of states was calculated using the 4×4×2 Monkhorst-Pack k-point.

The free energy was calculated using the equation:

$$G = E + ZPE - TS$$

Where, G , E , ZPE and TS represent the free energy, total energy from DFT calculations, zero point energy and entropic contributions, respectively.

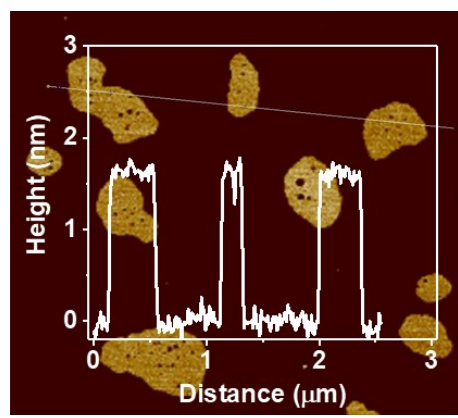


Fig. S1. AFM image and corresponding line-scan profiles of Fe, P–NiCH/CNTs.

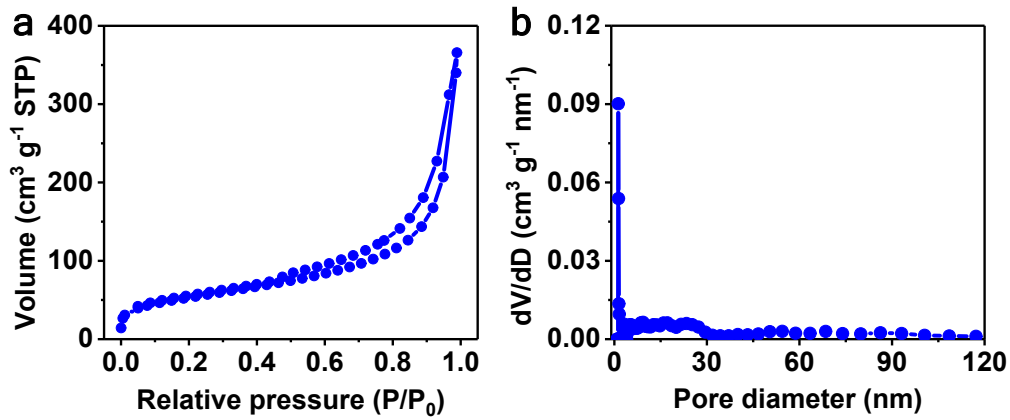


Fig. S2. (a) N₂ adsorption-desorption curves and (b) corresponding pore size distribution curves of Fe, P–NiCH/CNTs.

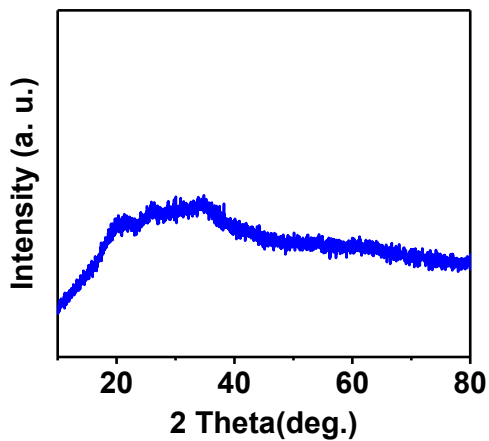


Fig. S3. XRD patterns of Fe, P–NiCH/CNTs.

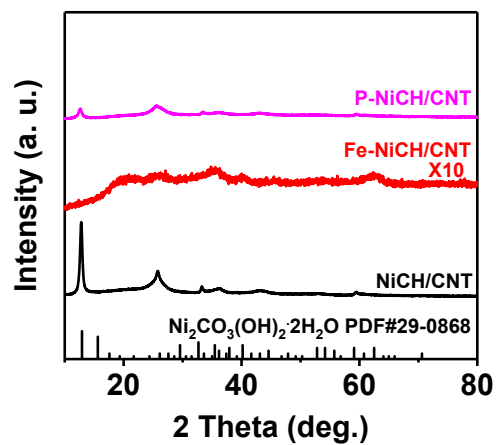


Fig. S4. XRD patterns of NiCH/CNTs, Fe–NiCH/CNTs and P–NiCH/CNTs.

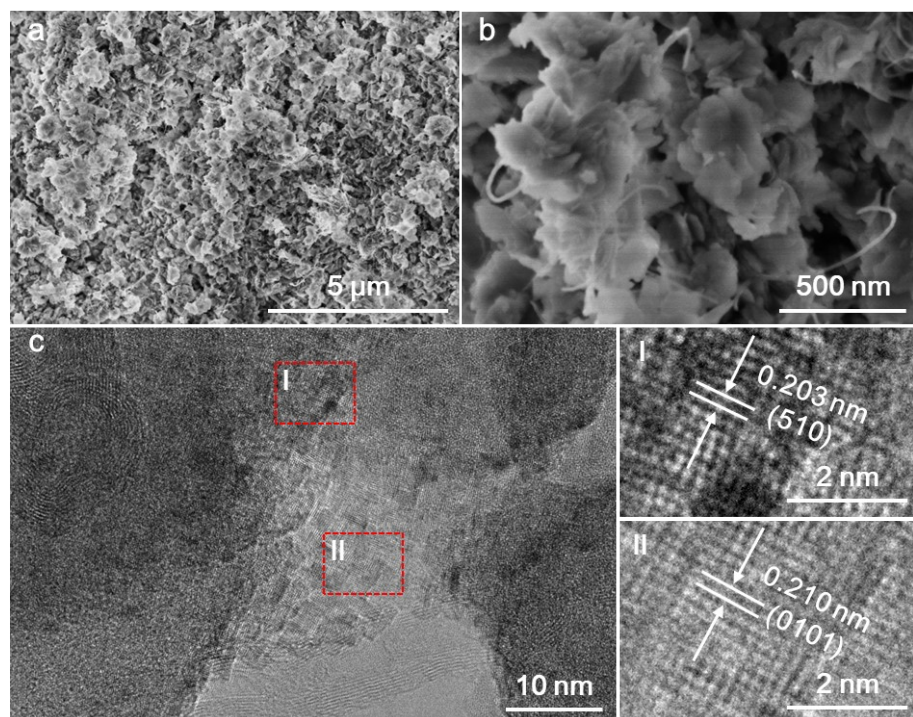


Fig. S5. (a) Low-, (b) high-magnification SEM images and (c) HRTEM image of NiCH/CNTs.

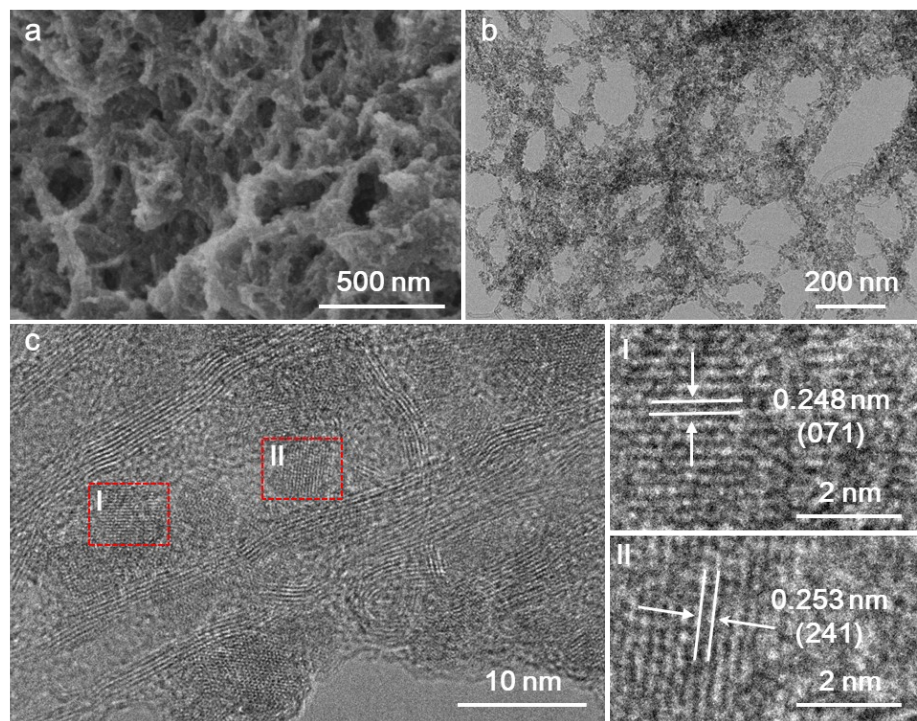


Fig. S6. (a) Low-, (b) high-magnification SEM images and (c) HRTEM image of Fe–NiCH/CNTs.

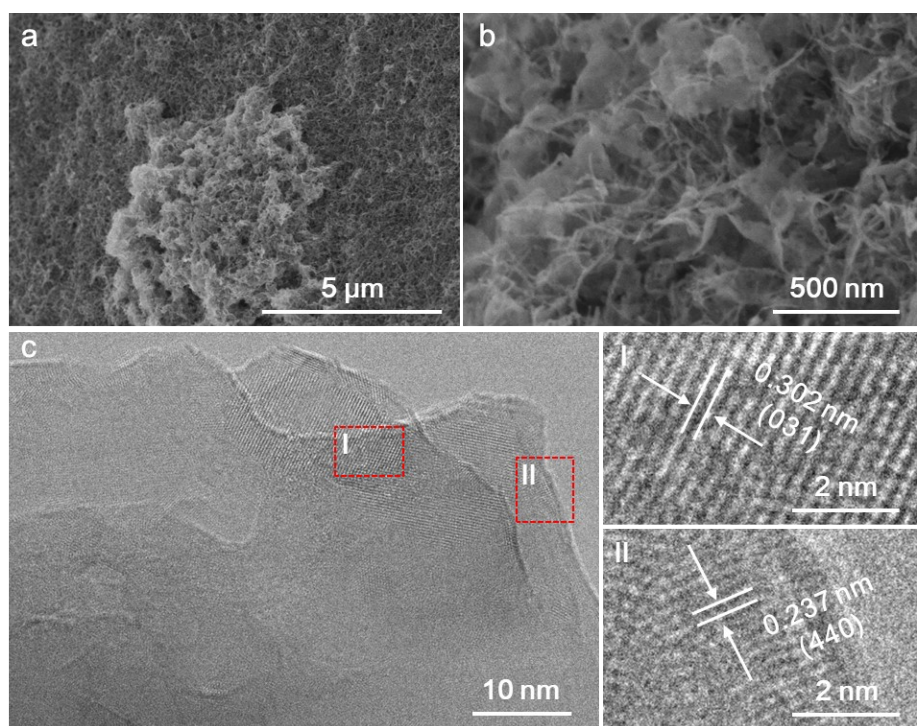


Fig. S7. (a) Low-, (b) high-magnification SEM images and (c) HRTEM image of P–NiCH/CNTs.

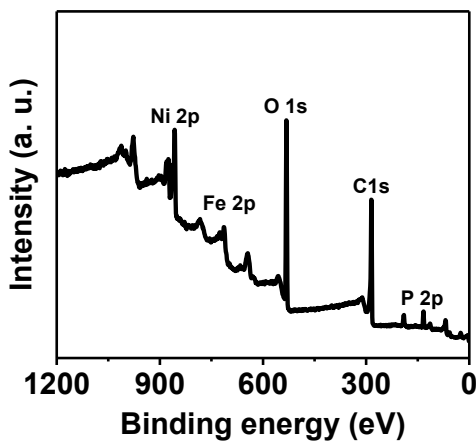


Fig. S8. XPS survey spectra of Fe, P–NiCH/CNTs.

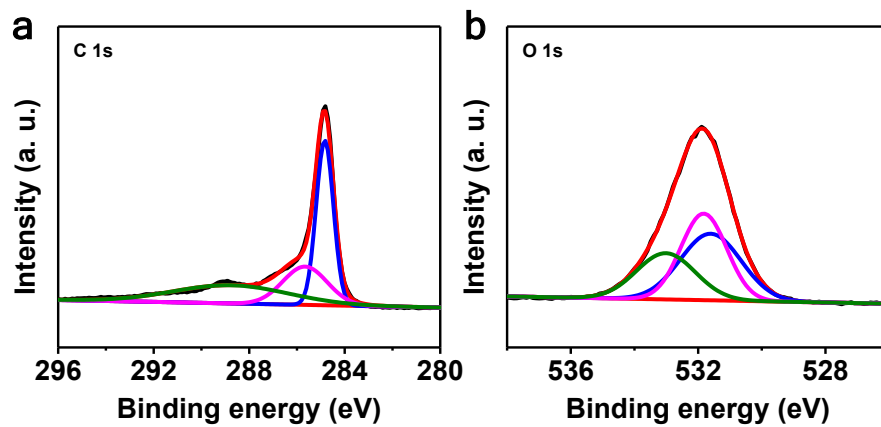


Fig. S9. (a) C 1s and (b) O 1s spectra of of Fe, P–NiCH/CNTs.

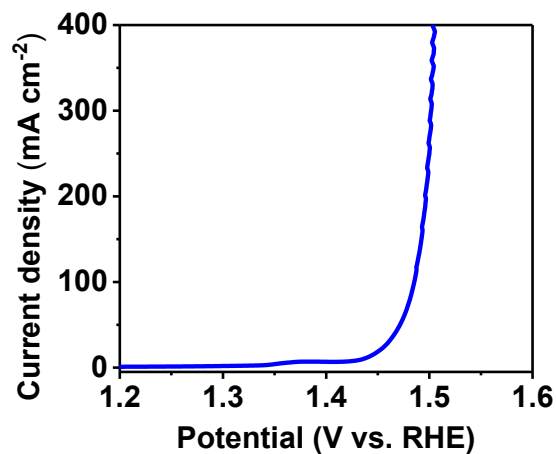


Fig. S10. LSV curves of Fe, P–NiCH/CNTs coated on the Ni foam surface.

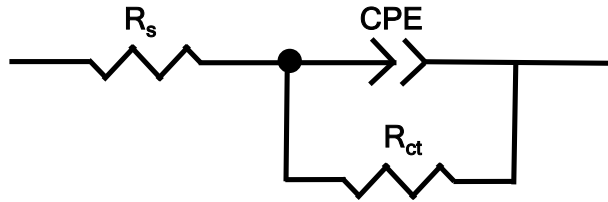


Fig. S11. The equivalent circuit model of EIS analysis of all samples.

The equivalent circuit is consisted by a parallel combination of (R_{ct} , CPE) element in series with R_s . The CPE represents as the double layer capacitor from the catalyst/support and catalyst solution. R_s and R_{ct} is the uncompensated solution resistance and charge transfer resistance arisen from the relevant electro-chemical oxidation, respectively.

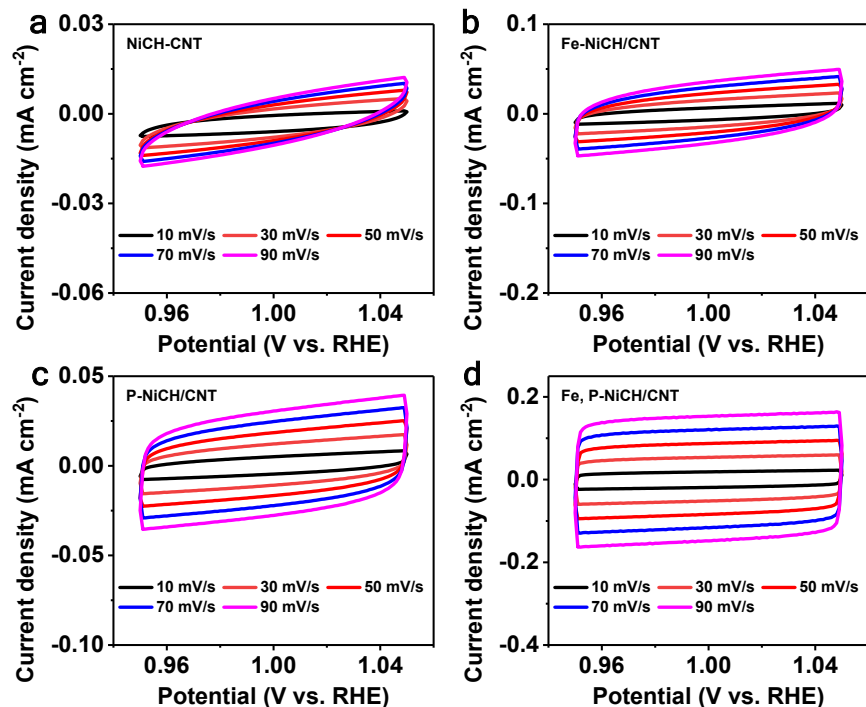


Fig. S12. CV curves of (a) NiCH/CNTs, (b) Fe–NiCH/CNTs, (c) P–NiCH/CNTs and (d) Fe, P–NiCH/CNTs at different scan rates.

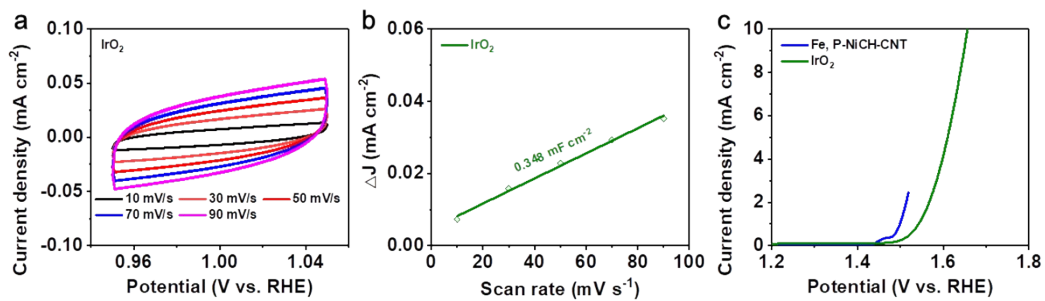


Fig. S13. (a) CV curves, (b) (d) C_{dl} , (e) ECSA-normalized LSV curves of IrO_2 .

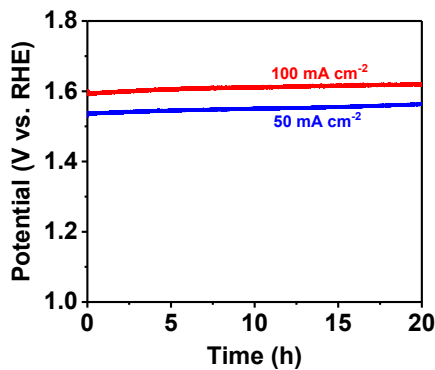


Fig. S14. The chronopotentiometry test curves of the Fe, P–NiCH/CNTs at 50 and 100 mA cm^{-2} .

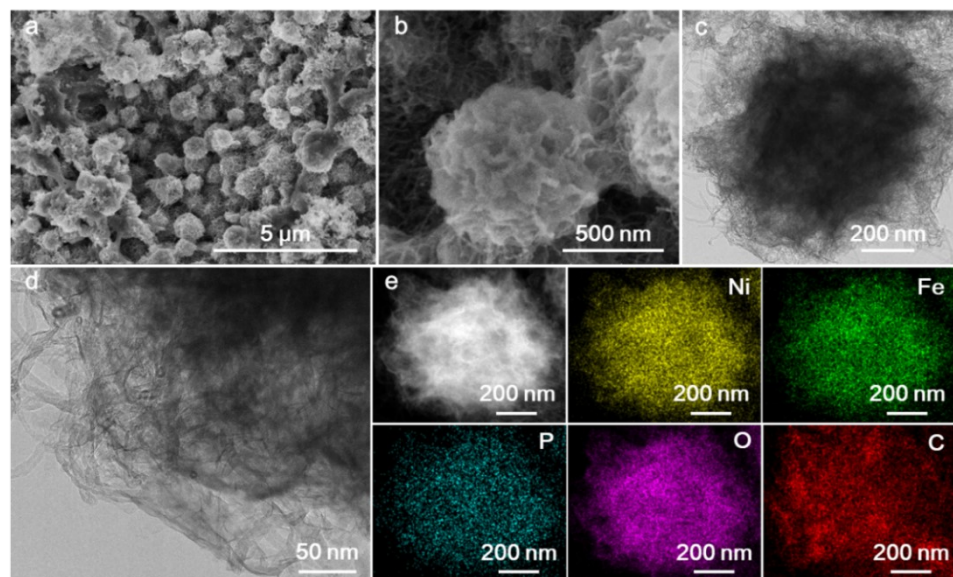


Fig. S15. Structural characterization of Fe, P–NiCH/CNTs after long-term OER measurement. (a) Low-, (b) high-magnification SEM images, (c) low-, (d) high-magnification TEM images and (e) HAADF-STEM image and corresponding element mapping.

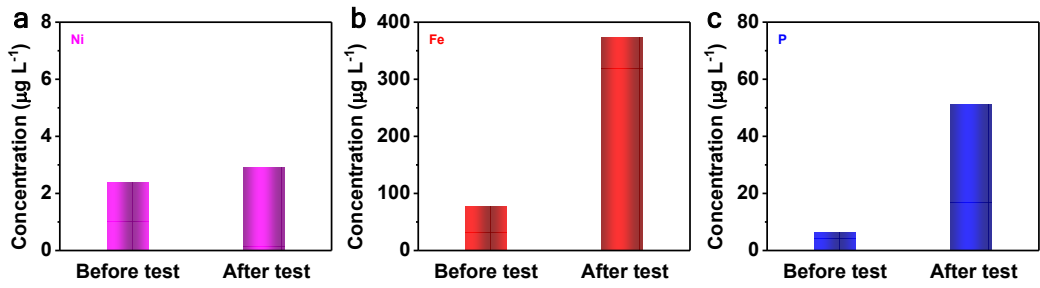


Fig. S16. Comparison of (a) Ni, (b) Fe and (c) P concentration in electrolyte before and after long-term OER measurement.

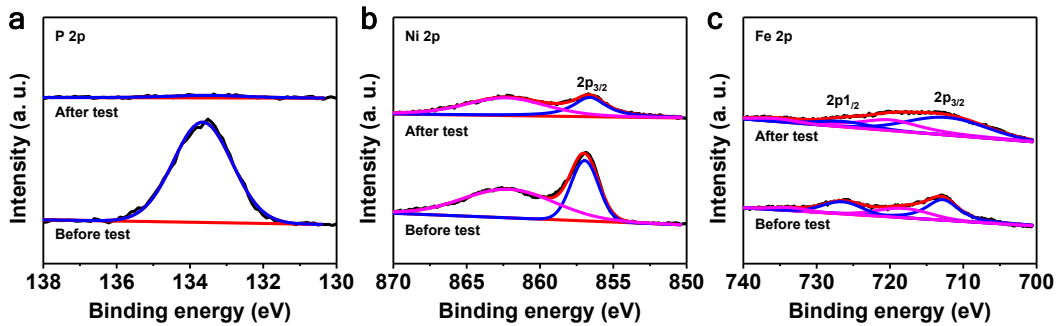


Fig. S17. Comparison of (a) P 2p, (b) Ni 2p and Fe 2p spectra of Fe, P–NiCH/CNTs before and after long-term OER test.

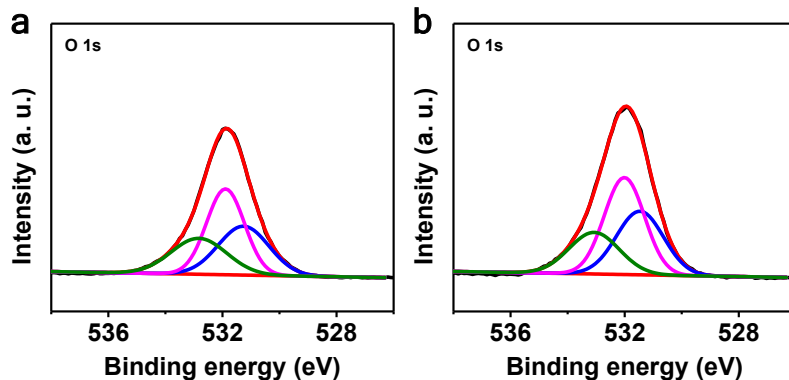


Fig. S18. O 1s spectra of Fe, P–NiCH/CNTs with higher (a) Fe and (b) P doping dosage.

Table S1 Comparison of OER activity of Fe, P–NiCH/CNTs with other reported carbonate hydroxides and nickel based OER electrocatalysts

Electrocatalysts	Current density (mA cm ⁻²)	Overpotential (mV)	References
Fe, P–NiCH/CNTs	20	222	This work
Ni_xFe_yS/CH	20	261	[1]
FCCH/NF	10	228	[2]
NiCoCHH/CC	10	238	[3]
NiFeHCH	20	250	[4]
C@NFeCoCH/CC	10	235	[5]
CoCO₃ PNSs	10	310	[6]
Fe_{0.25}–CoMoCH/NF	10	232	[7]
Co_{0.95}Mn_{0.05}CO₃/GP	10	266	[8]
(Ru-Ni)O_x/NF	10	237.2	[9]
NiO–Ni CHNAs/CFC	10	235	[10]
NiO/NiFe₂O₄/NF	10	290	[11]
NiSe₂/FeSe₂	10	256	[12]
Ni–Fe LDH nanocages	20	246	[13]
Ni₃N/Ni@Ni3N	20	229	[14]
Co_{1.6}Ni_{0.4}P₄O₁₂–C	10	230	[15]

Table S2 EIS fitting parameters from equivalent circuits during OER process

Samples	R _s /Ω	CPE/S s ⁻ⁿ	n/0<n<1	R _{ct} /Ω
NiCH/CNTs	7.57	4.50×10 ⁻⁶	0.850	1.67×10 ⁵
Fe–NiCH/CNTs	9.76	0.00285	0.664	664.9
P–NiCH/CNTs	15.52	0.00343	0.916	295.9
Fe, P –NiCH/CNTs	10.12	0.00846	0.881	11.2

References

- 1 Y. Yang, X. Luan, X. Dai, X. Zhang, H. Qiao, H. Zhao, J. Yong, L. Yu, J. Han

- and J. Zhang, *Electrochim. Acta*, 2019, **309**, 57-64.
- 2 L. Hui, Y. Xue, D. Jia, H. Yu, C. Zhang and Y. Li, *Adv. Energy Mater.*, 2018, **8**, 1800175.
 - 3 K. Karthick, S. Subhashini, R. Kumar, S. Sethuram Markandaraj, M. M. Teepikha and S. Kundu, *Inorg. Chem.*, 2020, **59**, 16690-16702.
 - 4 K. Karthick, S. Ananthraj, S. R. Ede and S. Kundu, *Inorg. Chem.*, 2019, **58**, 1895-1904.
 - 5 M. Dai, H. Fan, G. Xu, M. Wang, S. Zhang, L. Lu and Y. Zhang, *J. Power Sources*, 2020, **450**, 227639.
 - 6 Y. Jia, Y.-N. Li, Z.-M. Wang, F.-M. Li, P.-J. Jin, S.-N. Li and Y. Chen, *Chem. Eng. J.*, 2021, **417**, 128066.
 - 7 M. Cai, X. Lu, Z. Zou, K. Guo, P. Xi and C. Xu, *ACS Sustain. Chem. Eng.*, 2019, **7**, 6161-6169.
 - 8 A. Karmakar and S. K. Srivastava, *ACS Appl. Energy Mater.*, 2020, **3**, 7335-7344.
 - 9 H. Zhang, Y. Lv, C. Chen, C. Lv, X. Wu, J. Guo and D. Jia, *Appl. Catal. B-Environ.*, 2021, **298**, 120611.
 - 10 Y. Lei, T. Xu, S. Ye, L. Zheng, P. Liao, W. Xiong, J. Hu, Y. Wang, J. Wang, X. Ren, C. He, Q. Zhang, J. Liu and X. Sun, *Appl. Catal. B-Environ.*, 2021, **285**, 119809.
 - 11 H. Zhong, G. Gao, X. Wang, H. Wu, S. Shen, W. Zuo, G. Cai, G. Wei, Y. Shi, D. Fu, C. Jiang, L.-W. Wang and F. Ren, *Small*, 2021, **17**, 2103501.
 - 12 S. Ni, H. N. Qu, Z. H. Xu, X. Y. Zhu, H. F. Xing, L. Wang, J. M. Yu, H. Z. Liu, C. M. Chen and L. R. Yang, *Appl. Catal. B-Environ.*, 2021, **299**, 120638.
 - 13 J. Zhang, L. Yu, Y. Chen, X. F. Lu, S. Gao and X. W. D. Lou, *Adv. Mater.*, 2020, **32**, e1906432.
 - 14 X. R. Gao, X. M. Liu, W. J. Zang, H. L. Dong, Y. J. Pang, Z. K. Kou, P. Y. Wang, Z. H. Pan, S. R. Wei, S. C. Mu and J. Wang, *Nano Energy*, 2020, **78**, 105355.
 - 15 Y. Li, Z. Wang, J. Hu, S. Li, Y. Du, X. Han and P. Xu, *Adv. Funct. Mater.*, 2020, **30**, 1910498.